Decomposition of nitramine energetic materials in excited electronic states: RDX and HMX

Y. Q. Guo, M. Greenfield, and E. R. Bernstein

Citation: The Journal of Chemical Physics **122**, 244310 (2005); doi: 10.1063/1.1929741
View online: http://dx.doi.org/10.1063/1.1929741
View Table of Contents: http://aip.scitation.org/toc/jcp/122/24
Published by the American Institute of Physics

Decomposition of nitramine energetic materials in excited electronic states: RDX and HMX

Y. Q. Guo, M. Greenfield, and E. R. Bernstein[a)]
Department of Chemistry, Colorado State University, Fort Collins, Colorado 80523

(Received 7 March 2005; accepted 19 April 2005; published online 28 June 2005)

Ultraviolet excitation (8-ns duration) is employed to study the decomposition of RDX (1,3,5-trinitro-1,3,5-triazacyclohexane) and HMX (1,3,5,7-tetranitro-1,3,5,7-tetrazacyclooctane) from their first excited electronic states. Isolated RDX and HMX are generated in the gas phase utilizing a combination of matrix-assisted laser desorption and supersonic jet expansion techniques. The NO molecule is observed as one of the initial dissociation products by both time-of-flight mass spectroscopy and laser-induced fluorescence spectroscopy. Four different vibronic transitions of NO are observed: $A\,^2\Sigma(v'=0)\leftarrow X\,^2\Pi(v''=0,1,2,3)$. Simulations of the NO rovibronic intensities for the $A\leftarrow X$ transitions show that dissociated NO from RDX and HMX is rotationally cold ($\sim$20 K) and vibrationally hot ($\sim$1800 K). Another potential initial product of RDX and HMX excited state dissociation could be OH, generated along with NO, perhaps from a HONO intermediate species. The OH radical is not observed in fluorescence even though its transition intensity is calculated to be 1.5 times that found for NO per radical generated. The HONO intermediate is thereby found not to be an important pathway for the excited electronic state decomposition of these cyclic nitramines. © *2005 American Institute of Physics*.
[DOI: 10.1063/1.1929741]

I. INTRODUCTION

Energetic materials such as RDX (1,3,5-trinitro-1,3,5-triazacclohexane), HMX (1,3,5,7-tetranitro-1,3,5,7-tetraazacyclooctane), and other nitramines have been intensively investigated both theoretically[1–4] and experimentally[5–8] over the past several decades. In order to understand how shock waves and impact can initiate the rapid exothermic chemical reactions that lead to detonation in explosive solids, most of the previous studies have focused mainly on the ground electronic state in the condensed phase.[9–14] Study of these materials in the condensed phase, however, does not expose the difference between the intramolecular and intermolecular behaviors and the fundamental properties of these molecules. To understand the properties and reactions of energetic materials at a fundamental level, an elucidation of their molecular behavior is essential. Gas phase studies of these energetic materials can reveal the behavior of such molecular species.[15] Decomposition of RDX and HMX as isolated molecules in the gas phase can be determined as a function of electronic and vibrational state excitations. A reaction mechanism can be proposed and tested for the energetic molecules of interest by further disclosing which bonds rupture first and on what time scales.

Decomposition of energetic materials from the excited state plays a very important role in the overall decomposition mechanisms and kinetics.[5,16–19] One suggested mechanism of detonation initiation in the condensed phase is that of "hot spot" generation.[20] A hot spot is presumed to be a small region in a crystal that localizes the energy of an impact/shock wave and triggers the chemical reaction. Formation of hot spots is thought to involve electronic excitation; several proposed mechanisms for hot spot initiation are related to excited electronic states of energetic materials.[21,22]

Additionally, ignition processes, such as sparks, shocks, slow/rapid heating, lasers, and arcs, can all initiate the decomposition reaction of energetic materials by generating excited electronic states via excitonic and highest occupied molecular-orbital/lowest occupied molecular-orbital (HOMO/LUMO) gap molecular mechanisms.[23] These dissociative and reactive excited electronic states will then generate small radicals and atoms that initiate and propagate a series of ultrafast reactions and enhance the energy release process. Generation of gas phase species is possible in all the above initiation processes. As crystal planes shear, large electric fields propagate through the crystal and excite molecules. Only a few excited state molecules are needed to generate radicals and ions to begin the rapid decomposition process for the entire sample. Thus, the decomposition of solid energetic materials should involve both ground and excited electronic states, as well as both gas and condensed phase species.[24–26] An elucidation of the behavior of energetic nitramines for various applications should consider all of these circumstances and initial conditions. Therefore, isolated gas phase molecular investigations into the excited electronic states of HMX and RDX will yield an improved understanding of their molecular and condensed phase behaviors at a fundamental level.

To date, theoretical investigations of unimolecular HMX in the ground electronic state show decomposition mainly through two channels: N–N bond rupture to generate NO_2

[a)]Electronic mail: erb@lamar.colostate.edu

and HONO formation from a five-membered ring elimination reaction.[27–31] For unimolecular RDX, theoretical calculations suggest multiple decomposition pathways.[32–34] A few experimental gas phase, ground[35–37] and excited electronic state[38–41] studies are reported. These experimental studies suggest different mechanisms depending on the electronic state of RDX: N–N bond scission to generate NO_2,[40] ground electronic state concerted ring fission to generate three CH_2NNO_2 (Ref. 35) radicals, and loss of OH via a five-membered ring intermediate.[36,39] We have found that gas phase, isolated excited electronic state RDX generates NO as an initial product ($\sim$8 ns). NO_2 was eliminated as a possible reaction intermediate for this decomposition pathway through NO_2 decomposition studies.[38,42] RDX and HMX can generate NO through two reaction channels: loss of O and then N–N bond scission of the unstable nitrosamine intermediate $[(CH_2NNO_2)_2CH_2NNO]$ and HONO loss and then fragmentation of this species to yield both OH and NO in equal amounts. This latter channel would involve the formation of the intermediate RDX and HMX five-membered ring transition states […NN(O)O···CH…], as indicated in Fig. 1.

In this report, we continue to pursue the isolated molecule, excited electronic state decomposition pathways for RDX and HMX on an 8-ns time scale. RDX and HMX are excited to their first excited electronic states and NO is observed by laser-induced fluorescence (LIF) spectroscopy and time-of-flight mass spectroscopy (TOFMS). For both RDX and HMX NO is found to be rotationally cold ($\sim$20 K) and vibrationally hot ($\sim$1800 K). OH is not observed by LIF spectroscopy in the same experiments in which NO is observed. If HONO is the OH and NO precursor, the OH LIF signal should be 1.5 times as intense as the NO LIF signal. Thus we conclude that the five-membered ring elimination is not an important pathway for the decomposition of these energetic nitramines from the excited electronic state. In brief, the decomposition mechanism of RDX and HMX from their excited electronic states is apparently different than that from ground electronic states in either gas or condensed phase.

II. EXPERIMENTAL PROCEDURES

The combination of matrix-assisted laser desorption and supersonic jet expansion is employed to obtain a molecular beam of a nonvolatile, thermally unstable sample, such as an energetic nitramine, in a vacuum chamber. The experimental setup has been described in detail in our previous publication on TOFMS of RDX and NO.[38] In this section we will review, briefly, the main components of this apparatus and discuss the LIF addition to the detection procedure for OH and NO. The nozzle employed for the sample beam generation is constructed from a Jordan Co. pulsed valve and a laser ablation attachment: the system is modeled after a design by Smalley[43] and is discussed in Refs. 44 and 45. The laser desorption head is attached to the front of the pulsed valve and consists of a 2×60-mm^2 channel for the expansion gas from the nozzle, a conical channel (3 mm at the outside and 1 mm at the intersection with the expansion gas channel) for the ablation laser beam perpendicular to the expansion gas channel, and a ca. 40-mm diameter hole for the sample drum. The sample drum tangentially intersects the expansion gas channel near the middle of the laser desorption head, at the intersection of the ablation laser conical channel and the expansion gas channel. The sample drum fits into the 40-mm hole and is simultaneously rotated and translated, by a motor and gear system operating in vacuum, to present a fresh sample region to the ablation laser for each few pulses. The sample drum is electrolytically[46–49] coated with a microscopically rough, porous surface of Al_2O_3 prior to sample deposition on the drum. A solution of equimolar amounts of sample (RDX/HMX) and matrix (R6G) in acetone is uniformly sprayed on the drum surface while it is rotating under a heat lamp in a fume hood. The dried drum is then placed in the laser ablation head/nozzle assembly and put into a vacuum chamber for LIF or TOFMS detection of RDX/HMX decomposition products. Under microscopic examination, the deposited sample is noncrystalline, uniformly red, and completely covers the microscopically rough Al_2O_3 surface. The nitramine molecules are desorbed from the drum by laser ablation at 532 nm, entrained in the flow of He carrier gas through the 2×60-mm^2 channel in the ablation head, and expanded into the vacuum chamber. Two chambers are used: a TOFMS and an LIF chamber, both of which have been previously described.[38,50–52] This procedure has been employed to detect NO for both RDX and HMX by LIF or TOFMS.

The Al_2O_3 matrix generates a very strong OH signal in LIF spectroscopy and so the matrix preparation procedure must be modified to detect OH from the energetic nitramine alone. In this instance we find that a piece of porous filter paper attached to an Al metal-surface drum gives no OH signal but that, due to the reduced roughness (surface area) of the paper with respect to the Al_2O_3 coating, the sample/matrix ratios must be changed from 1:1 to 2:1.

In addition to the 532-nm ablation laser, one or two additional lasers are required to photoexcite the nitramine energetic material in the beam and then detect the fragmented small species (either NO or OH in this case). For NO detection, a single pump/probe laser is needed at 226–258 nm to both initiate dissociation of RDX and HMX and detect NO through LIF or TOFMS $[A(v'=0)\leftarrow x(v''=0\text{-}3)$ and $I\leftarrow A]$. For LIF detection of OH, two lasers are required: one at 226 nm to fragment RDX or HMX; and one at 308 nm to detect OH by LIF.

The three laser beams enter the LIF chamber by three different windows. The 226-nm photoexcitation pump laser and the 308-nm detection/probe laser for OH counter propagate and intersect the molecular beam perpendicularly at ca. 2 cm from the face of the ablation head/nozzle structure. These lasers are focused by 2- and 1.5-m lenses, respectively, at the beam intersect position. The UV energy ranges from 0.2 to 0.6 mJ/pulse and, at the 0.5-mm focal point, the intensity of the laser beams is in the range $\sim$3 to $\sim8\times10^6$ W/cm^2 for an 8-ns pulse duration.

In both the LIF and TOFMS experiments the timing sequence for the pulsed nozzle and lasers is controlled by time delay generators (SRS DG535). The experiment is conducted at a repetition rate of 10 Hz. Ion signals, in the TOFMS, are

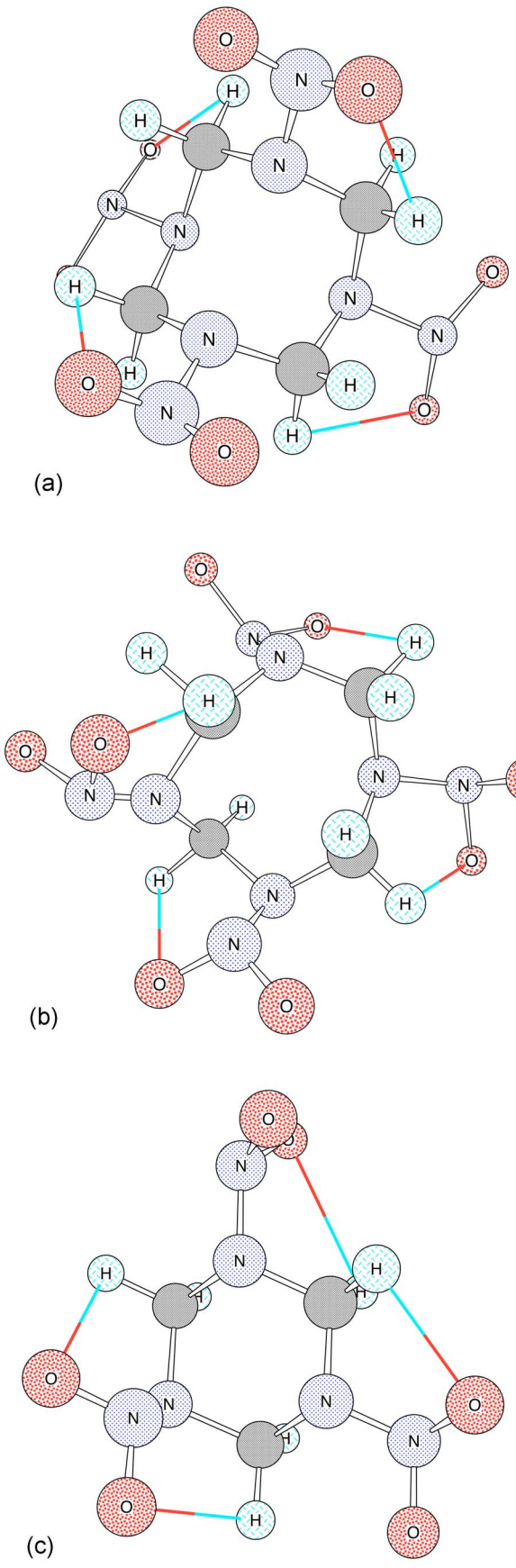

FIG. 1. (a) δ-HMX with possible H–O bonds to form five-membered ring. Oxygen (red), nitrogen (blue), carbon (gray), hydrogen (aqua), possible hydrogen–oxygen bonds are two color (red and aqua). (b) β-HMX with possible H–O bonds to form five-membered ring. (c) RDX with possible H–O bonds to form five-membered rings.

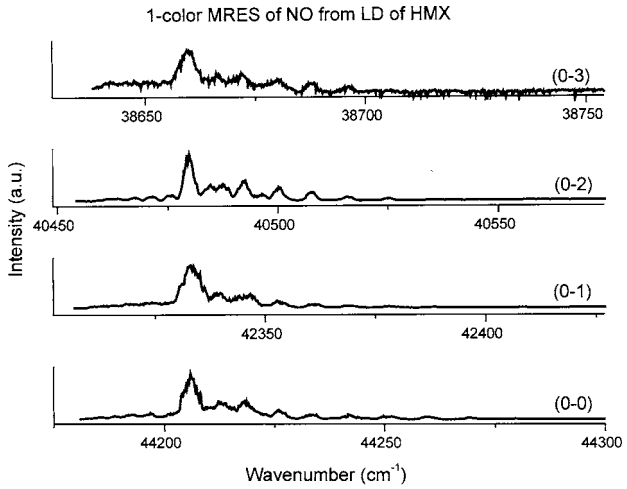

FIG. 2. NO spectra $A(v'=0) \leftarrow X(v''=0,1,2,3)$. NO is generated from the photodissociation of HMX.

detected by a microchannel plate (MCP) detector and fluorescence signals are detected by a RCA C31034 photomultiplier tube. Signals are recorded and processed on a personal computer (PC) using an ADC card (Analog Devices RTI-800) and a boxcar averager (SRS SR 250). In all experiments the chamber pressure and pulsed valve timing remain constant. For the ion velocity slip measurements, the fragment/ionization laser timing is swept.

III. RESULTS AND DISCUSSION

Figure 2 shows the spectra of four different $A(v'=0) \leftarrow X(v''=0,1,2,3)$ rovibronic transitions of the NO molecule generated from laser-desorbed HMX excited to its first excited electronic state. All spectra show nearly the same rotational pattern but have a different vibronic intensity for each band. The intense feature in each spectrum is assigned as the $(Q_{11}+P_{21})$ band and the lower intensity features for each vibronic transition are other rotational transitions.[53,54]

The top spectrum in Fig. 3 is the (0-1) transition for NO derived from laser-desorbed RDX photodissociation, and the

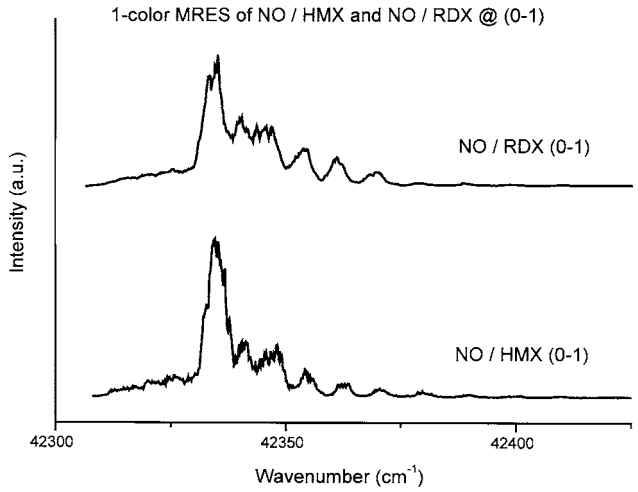

FIG. 3. Comparison of NO spectra $[A(v'=0) \leftarrow X(v''=1)]$ between NO/HMX (bottom) and NO/RDX (top).

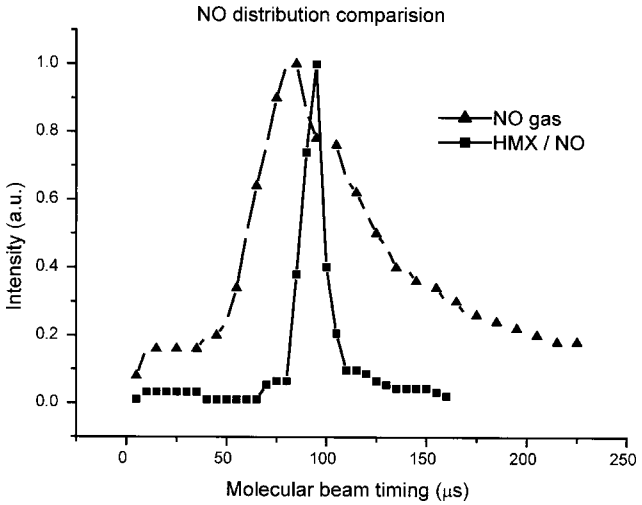

FIG. 4. A comparison between the detected distributions of NO TOFMS intensity from two different sources: (1) gas phase NO expanded through a supersonic nozzle (triangles), and (2) gas phase NO derived from MALD generated HMX fragmented at the TOFMS ion source region (squares).

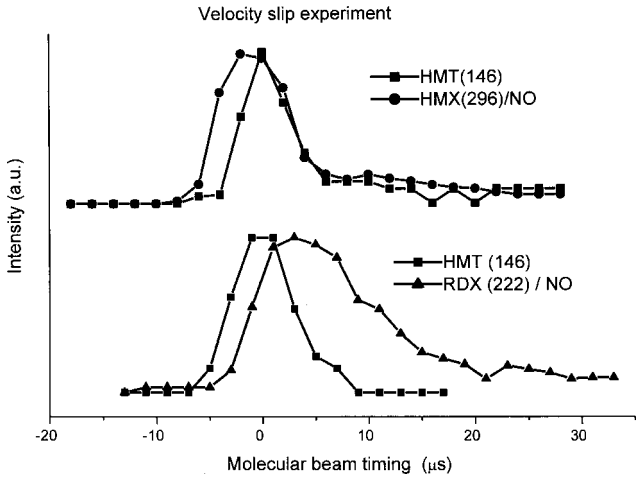

FIG. 5. Velocity distribution differences between laser-desorbed HMT and RDX (bottom) or HMX (top). Equimolar quantities of HMT and RDX/HMX samples are coated together with the matrix molecule R6G. Signals from the parent molecule for HMT, NO for RDX/HMX have been used to determine the velocity distribution data. The precise relative arrival time for HMT and RDX/HMX is determined by molecular mass and collision cross section (see text for more discussion).

bottom spectrum of Fig. 3 is for NO derived from laser-desorbed and photodissociated HMX. Careful comparison between the two spectra shows that they are equivalent; this suggests that the decomposition pathway to the NO product is the same for both excited RDX and HMX.

Even though the matrix-assisted laser desorption technique is known to place easily fragmented, fragile molecules in the gas phase without fragmentation,[55,56] one must still ensure that RDX/HMX is not fragmented in the ablation process. That is, we must try to demonstrate that laser ablation at 532 nm (RDX/HMX does not absorb at this wavelength, while the R6G matrix does) does not generate NO in the nozzle that is then cooled in the expansion process. We must distinguish between NO generated in the nozzle by the ablation laser and NO generated at the decomposition/ionization/LIF region by the pump/probe lasers. This distinction was made for RDX at great length in our previous study, in which we also demonstrated that NO_2 was not a precursor for NO.[38,42] Here we briefly present three methods for making this determination: comparison of NO velocity distributions from the nozzle, determination of arrival time for the NO signal intensity as a function of nozzle/pump laser timing (velocity slip measurement), and NO rotational and vibrational temperature determinations as a function of source of NO.

Figure 4 shows that the gas phase NO signal (1%NO/99%He) from the nozzle has a much different distribution than the HMX/NO signal. Therefore, the NO signal attributed to HMX is not background NO from the nozzle expansion gas. This figure also demonstrates that the NO does not diffuse into the expansion gas after ablation, as could be anticipated for a light molecule. Thus, this result suggests that HMX is not photodissociated in the ablation process.

Figure 5 presents data on the arrival times for NO signals derived from RDX and HMX at the ionization region of the TOFMS relative to the heavy molecule HMT [hexamethylene tetramine - $(CH_2)_6N_4=C_6H_{12}N_4$]. Both sources for the NO^+ signal have an arrival time of a heavy molecule compared to NO. A slower speed for heavy molecules in the expansion (velocity slip) is related to the molecules' mass and collision cross section,[44,45,57,58] therefore HMT, RDX, and HMX arrive at the ionization region from the nozzle much later than a light molecule such as NO does.[38]

Finally, one can characterize the rotational and vibrational temperatures (T_{rot} and T_{vib}, respectively) for NO under different sample and generation conditions: (1) NO mixed with the backing gas at ca. 1% in He and (2) NO derived from laser ablated RDX/HMX fragmented at the ionization region of the TOFMS or the LIF point in the low-density molecular beam. At the NO (0-0), $T_{rot} \sim 11$ K for 100-psi expansion and $\sim 1\%$NO/99%He. This is rotationally colder than (0-0) NO from RDX or HMX for which $T_{rot} \sim 20$ K. On the other hand, T_{rot} for NO (0-1) mixed into the backing gas under these conditions is ca. 100 K, while NO from RDX and HMX remains ca. 20 K (see Fig. 6). No NO (0-2,3) transitions are observed for NO mixed into the backing gas, while RDX and HMX produce (0-0), (0-1), (0-2), and (0-3) vibronic transitions with a $T_{vib} \sim 1800$ K and $T_{rot} \sim 20$ K.

These three observations, taken together, prove that NO is a primary decomposition product of RDX and HMX at the pump/probe laser access point in the ionization region of the TOFMS. The above observations are completely consistent with the LIF results. On the contrary, if the NO were generated in the nozzle by laser ablation it would have to be generated with a very cold rotational temperature and a very hot vibrational temperature that were not changed in the supersonic expansion. We consider this highly unlikely, but still indicative of the decomposition of RDX and HMX from their excited electronic states. According to the above analysis, the NO molecule is demonstrated to be an initial product of the decomposition of RDX and HMX from an isolated, excited electronic state molecule. As pointed out in the Introduction, NO has been shown not to derive from the N–N

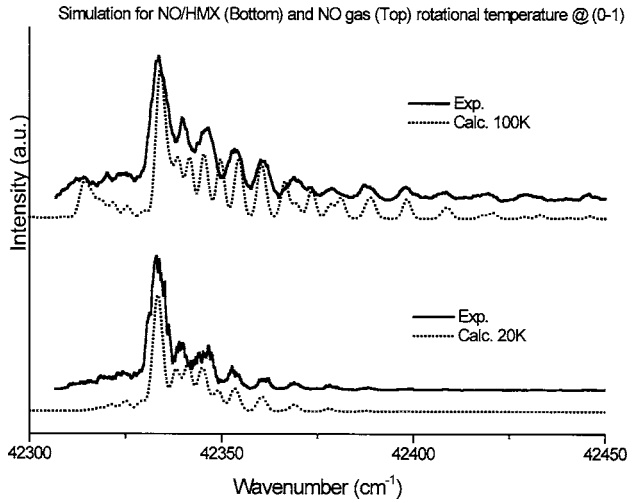

FIG. 6. Simulations of the NO rotational spectra at the (0-1) transition obtained from photodissociation of HMX (bottom) and NO gas (top). The dotted lines are the simulated spectra fit to the experimental spectra (solid line). The rotational temperatures for NO/HMX and NO gas are determined to be 20 and 100 K, respectively.

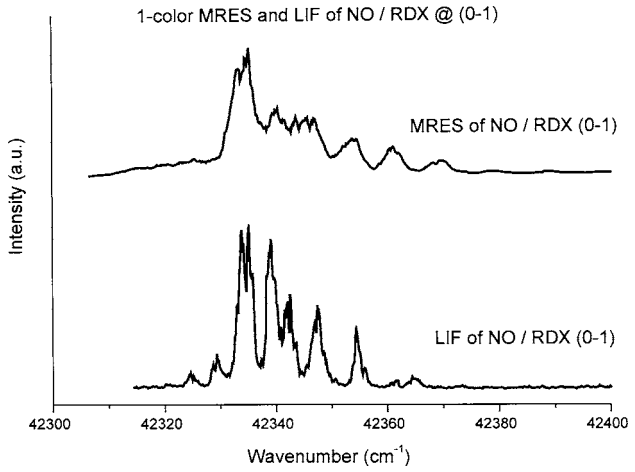

FIG. 7. MRES (top) and LIF spectrum (bottom) of NO (0-1) transition from NO fragmented from RDX photolysis.

bond scission product NO_2.[38,42] Another possible precursor of NO would be HONO derived from a five-membered ring formation with N–N–O···H–C connectivity in the intact nitramine or from concerted ring fission to form CH_2NNO_2 and again five-membered ring connectivity. Assuming that HONO is the intermediate in the formation of NO from RDX/HMX, one should observe OH at a comparable intensity to NO. Without such a pairing of OH and NO signals, the NO must arise from loss of O and formation of an unstable nitrosamine [...$H_2CN(NO)$...], which subsequently undergoes N–N bond scission to yield NO and $(CH_2N_2O_2)_2CH_2N$... .

The OH radical cannot be detected by TOFMS through multiphoton, stepwise absorption because the yield of OH^+ is quite small and the ionization energy for OH is 13.2 eV. LIF of OH is, however, well known and quite intense. Thus we can detect both NO and OH by LIF, to identify and observe OH and to confirm the TOFMS results for NO. The NO signal also serves as a standard signal by which one can calibrate the apparatus and the OH signal. Figure 7 illustrates the RDX NO TOFMS and LIF spectra and compares them for the (0-1) $A \leftarrow X$ transition. Although the LIF spectrum exhibits a narrower linewidth ($\sim 2\ cm^{-1}$) compared to the TOFMS linewidth ($\sim 5\ cm^{-1}$), both spectra are consistent with regard to T_{rot} and T_{vib}, based on spectral simulations. The slightly broader TOFMS linewidth than the LIF linewidth is probably due to power broadening of the TOFMS spectrum as three photons are required to generate this spectrum, and thus the focus is tighter and the intensity of the laser electric field is higher for the TOFMS detected spectrum. If HONO is the intermediate precursor to both OH and NO from these excited electronic state cyclic nitramines, the NO:OH emission ratio should be roughly 1:1.5 based on Franck-Condon factors and oscillator strengths for the respective $A \leftarrow X$ vibronic transitions. An average transition intensity for NO $A \leftarrow X$ (0-0) is ca. 200 mV on an oscilloscope. One should expect therefore to find a 300-mV OH detected signal. No such signal is observed for OH at maximum gain on the phototube. This result is in agreement with that of Ref. 36.

IV. CONCLUSIONS

NO is observed as an initial product of 8-ns UV single photon photodissociation of HMX and RDX. NO from this process is vibrationally hot and rotationally cold. OH is not observed by LIF detection and this eliminates HONO as an intermediate precursor for NO generation. The decomposition mechanism of RDX and HMX from their excited electronic states is apparently different than that from ground electronic states in either gas or condensed phase. Further investigations are presently underway to study the NO generation from RDX and HMX with 50-fs time resolution.

ACKNOWLEDGMENTS

These studies are supported in part by a DOD DURIP grant and a grant from US ARO and by the U.S. Department of Energy through the High Explosive Sciences Program at Los Alamos National Laboratory.

[1] W. Fickett and W. C. Davis, *Detonation* (University of California Press, Los Angeles, 1979).
[2] F. H. Ree, J. Chem. Phys. **81**, 1251 (1984).
[3] Y. Kohno, K. Ueda, and A. Imamura, J. Phys. Chem. **100**, 4701 (1996).
[4] D. C. Sorescu, B. M. Rice, and D. L. Thompson, J. Phys. Chem. B **102**, 6692 (1998).
[5] F. J. Owens and J. Sharma, J. Appl. Phys. **51**, 1494 (1979).
[6] S. Bulusu, D. I. Weinstein, J. R. Autera, and R. W. Velicky, J. Phys. Chem. **90**, 4121 (1986).
[7] J. J. Dick, R. N. Mulford, W. J. Spencer, D. R. Pettit, E. Garcia, and D. C. Shaw, J. Appl. Phys. **70**, 3572 (1991).
[8] J. C. Oxley, A. B. Kooh, R. Szekers, and W. Zhang, J. Phys. Chem. **98**, 7004 (1994).
[9] T. B. Brill and P. J. Brush, Philos. Trans. R. Soc. London, Ser. A **339**, 377 (1992).
[10] R. Behrens, Int. J. Chem. Kinet. **22**, 135 (1990).
[11] R. Behrens, S. Mack, and J. Wood, *JANNF 17th Propulsion Systems Hazards Subcommittee*, 1998 (unpublished), Vol. 1, p. 21.
[12] R. Behrens and S. Bulusu, Mater. Res. Soc. Symp. Proc. **418**, 119 (1996).
[13] M. R. Manaa, L. E. Fried, C. F. Melius, M. Elstner, and Th. Frauenheim, J. Phys. Chem. **106**, 9024 (2002).

[14] E. F. C. Byrd, G. E. Scuseria, and C. F. Chabalowski, J. Phys. Chem. **108**, 13100 (2003).
[15] A. N. Ali, S. F. Son, B. W. Asay, and R. K. Sander, J. Appl. Phys. **97**, 1 (2005).
[16] J. Sharma and B. C. Beard, in *Structures and Properties of Energetic Materials*, MRS Symposium Proceedings, edited by D. H. Liedenberg, R. W. Armstrong, and J. J. Gilman (MRS Pittsburgh, Pennsylvania, 1993).
[17] J. J. Gilman, Chem. Propulsion Inf. Agency **589**, 379 (1992).
[18] B. P. Aduev, E. D. Aluker, G. M. Belokurov, and A. G. Krechetov, Chem. Phys. Rep. **16**, 1479 (1997).
[19] A. B. Kunz, M. M. Kuklja, T. R. Botcher, and T. P. Russell, Thermochim. Acta **384**, 279 (2002).
[20] F. P. Bowden and Y. D. Yoffe, *Initiation and Growth of Explosion in Liquids and Solids* (Cambridge University Press, London, 1952), pp. 64–65.
[21] A. N. Dremin, Chem. Phys. Rep. **14**, 1851 (1995).
[22] J. J. Gilman, Philos. Mag. B **79**, 643 (1999).
[23] E. R. Bernstein, in *Overviews of Recent Research on Energetic Materials*, edited by D. Thompson, T. Brill, and R. Shaw (World Scientific, New Jersey, 2004).
[24] J. Sharma and B. C. Beard, Mater. Res. Soc. Symp. Proc. **296**, 189 (1993).
[25] T. R. Botcher, H. D. Landouceur, and T. R. Dussel, *Shock Compression of Condensed Matter-1997*, Proceedings of the Conference of the APS Topical Group No. 429, edited by S. C. Schimdt, D. P. Dankebar, and J. W. Forbes (1998), p. 989.
[26] B. P. Aduev, E. D. Aluker, and A. G. Krechetov, Chem. Phys. Rep. **17**, 469 (1998).
[27] Y. Oyumi and T. B. Brill, Combust. Flame **62**, 213 (1985).
[28] J. P. Lewis, Chem. Phys. Lett. **371**, 588 (2003).
[29] S. Zhang and T. N. Truong, J. Phys. Chem. A **105**, 2427 (2001).
[30] D. Chakraborty, R. P. Muller, S. Dasgupta, and W. A. Goddard, J. Phys. Chem. A **105**, 1302 (2001).
[31] J. P. Lewis, K. R. Glaesemann, K. VanOpdorp, and G. A. Voth, J. Phys. Chem. A **104**, 11384 (2000).
[32] D. Chakraborty, R. P. Muller, S. Dasgupta, and W. A. Goddard, J. Phys. Chem. A **104**, 2261 (2000).
[33] C. J. Wu and L. E. Fried, J. Phys. Chem. A **101**, 8675 (1997).
[34] T. D. Sewell and D. L. Thompson, J. Phys. Chem. **95**, 6228 (1991).
[35] X. Zhao, E. J. Hintsa, and Y. T. Lee, J. Chem. Phys. **88**, 801 (1988).
[36] H. Zuckermann, G. D. Greenblatt, and Y. Hass, J. Phys. Chem. **91**, 5159 (1987).
[37] T. A. Litzinger, B. L. Fetherolf, Y.-J. Lee, and C.-J. Tang, J. Propul. Power **11**, 698 (1995).
[38] H.-S. Im and E. R. Bernstein, J. Chem. Phys. **113**, 7911 (2000).
[39] C. Capellos, P. Papagiannakopoulos, and Y.-L. Liang, Chem. Phys. Lett. **164**, 533 (1989).
[40] C. Capellos, S. Lee, S. Bulusu, and L. Gams, *Advances in Chemical Reaction Dynamics* (Reidel, Dordrecht, 1986), pp. 398–404.
[41] C. Capellos, *12th International Detonation Symposium*, edited by J. M. Short and J. L. Maienschein (OCNR, Arlington, CA, 2003), p. 813.
[42] H.-S. Im and E. R. Bernstein, J. Phys. Chem. A **106**, 7565 (2002).
[43] R. E. Smalley, Laser Chem. **2**, 167 (1983).
[44] M. Foltin, G. J. Stueber, and E. R. Bernstein, J. Chem. Phys. **114**, 8971 (2001).
[45] M. Foltin, G. Stueber, and E. R. Bernstein, J. Chem. Phys. **111**, 9577 (1999).
[46] G. P. Wirtz, S. D. Brown, and W. M. Kriven, Mater. Manuf. Processes **6**, 87 (1991).
[47] P. Kurze, W. Krysmann, J. Schreckenbach, Th. Schwarz, and K. Rabending, Cryst. Res. Technol. **22**, 53 (1987).
[48] W. Krysmann, R. Kurze, K.-H. Dittrich, and H. G. Schneider, Cryst. Res. Technol. **19**, 973 (1984).
[49] K.-H. Dittrich, W. Krysmann, P. Kurze, and H. G. Schneider, Cryst. Res. Technol. **19**, 93 (1984).
[50] Q. Y. Shang and E. R. Bernstein, Chem. Rev. (Washington, D.C.) **94**, 2015 (1994).
[51] E. R. Bernstein, Annu. Rev. Phys. Chem. **46**, 197 (1995).
[52] E. R. Bernstein, *Atomic and Molecular Clusters*, edited by E. R. Bernstein (Elsevier, New York, 1990), p. 551.
[53] M. Hippler and J. Pfab, Chem. Phys. Lett. **243**, 500 (1995).
[54] G. Herzberg, *Spectra of Diatomic Molecules* (Van Nostrand, New York, 1950), p. 257.
[55] P. Carcabal, R. T. Kroemer, L. C. Snoek, J. P. Simons, J. M. Bakker, I. Compagnon, G. Meijer, and G. von Helden, Phys. Chem. Chem. Phys. **6**, 4546 (2004).
[56] L. C. Snoek, T. Van Mourik, and J. P. Simons, Mol. Phys. **101**, 1239 (2003).
[57] Q. Y. Shang, P. O. Moreno, S. Li, and E. R. Bernstein, J. Chem. Phys. **98**, 1876 (1993).
[58] Y. Matsuda, D. N. Shin, and E. R. Bernstein, J. Chem. Phys. **120**, 4142 (2004); Y. Matsuda and E. R. Bernstein, J. Phys. Chem. A **109**, 314 (2005).